An Aerial-Ground Robotic Team for Systematic Soil and Biota Sampling in Estuarine Mudflats

Pedro Deusdado[1], Eduardo Pinto[2], Magno Guedes[1], Francisco Marques[2], Paulo Rodrigues[2], André Lourenço[2], Ricardo Mendonça[2], André Silva[1], Pedro Santana[3,4], José Corisco[5], Marta Almeida[5], Luís Portugal[6], Raquel Caldeira[1], José Barata[2] and Luis Flores[1]

[1] INTROSYS SA, Portugal
[2] CTS-UNINOVA, Universidade Nova de Lisboa (UNL), Portugal
[3] ISCTE - Instituto Universitário de Lisboa (ISCTE-IUL), Portugal
[4] Instituto de Telecomunicações (IT), Portugal
[5] Centro de Ciências e Tecnologias Nucleares (C2TN), Instituto Superior Técnico, Universidade de Lisboa, Portugal
[6] Agência Portuguesa do Ambiente (APA), Portugal

Abstract. This paper presents an aerial-ground field robotic team, designed to collect and transport soil and biota samples in estuarine mudflats. The robotic system has been devised so that its sampling and storage capabilities are suited for radionuclides and heavy metals environmental monitoring. Automating these time-consuming and physically demanding tasks is expected to positively impact both their scope and frequency. The success of an environmental monitoring study heavily depends on the statistical significance and accuracy of the sampling procedures, which most often require frequent human intervention. The bird's-eye view provided by the aerial vehicle aims at supporting remote mission specification and execution monitoring. This paper also proposes a preliminary experimental protocol tailored to exploit the capabilities offered by the robotic system. Preliminary field trials in real estuarine mudflats show the ability of the robotic system to successfully extract and transport soil samples for offline analysis.

Keywords: Multi-Robot System, Field Robots, UGV, UAV, Environmental Monitoring, Radiological Monitoring, Estuarine Mudflats

1 Introduction

Primary deposition of contaminants, like radionuclides and heavy metals, on underwater surface sediments can occur through physical settling of particulate matter or through direct chemical sorption from the water. The process is ruled by physical conditions, such as water turbulence, contact time, sediment surface topography, and by the chemical nature and physical form of contaminants in the water column. All of these variables tend to be spatially complex, leading to heterogeneous distribution patterns of contaminants. In time, the hydrodynamics-induced redistribution of particles will intensify the spatial heterogeneity created by a primary deposition.

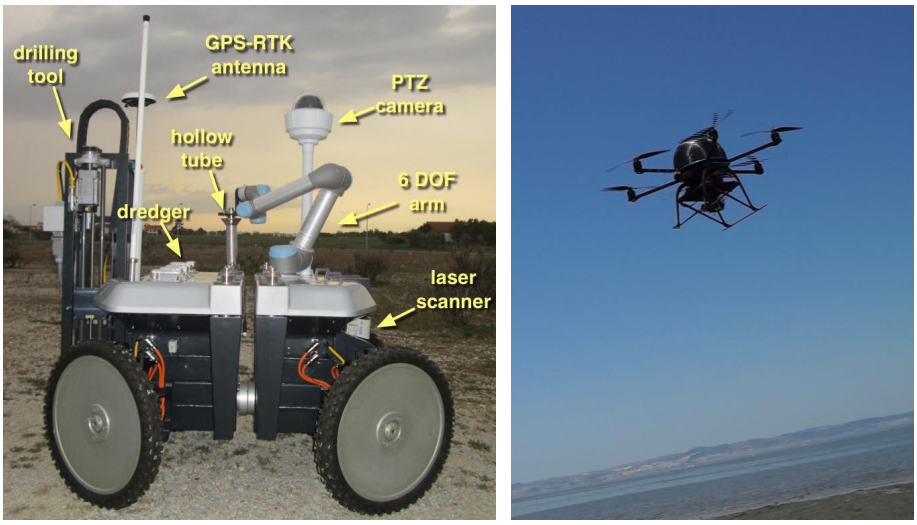

(a) (b)

Fig. 1. The robotic system. (a) The unmanned ground vehicle turning around its geometric centre. The robotic arm is moving a sample container to the drilling tool. (b) The UAV taking off for an aerial survey in the Samouco region.

The presence of radionuclides and heavy metals in the mudflats of estuarine bays may be an issue of increased public concern and environmental relevance, suggesting the need for an extensive survey of the intertidal mudflat. Continuous dredging of the navigation channel and fishery activities, such as intensive clam harvesting, promote the re-suspension of both surface and anoxic bottom sediments, which might be a cause for remobilisation of adsorbed toxicants [1].

Traditionally, surveys in estuarine mudflats are performed by experts who handle manual sampling tools and carry the samples from the site to the lab for an offline analysis. Walking in the mudflat, handling the sampling tools, transporting the samples, and ensuring those are properly tagged and geo-referenced, are just a few of the several physically demanding, costly, and time-consuming challenges humans must face in these sampling campaigns. To mitigate these difficulties, this paper presents a robotic system (see Fig. 1) developed to support sampling operations in mudflats and, as a result, facilitate thorough spatio-temporal sampling campaigns therein.

Robotic radiological monitoring is most often considered from an emergency-response perspective [2]. Conversely, the robotic team herein presented targets routine radiologic monitoring campaigns. The robotic system is composed of a wheeled Unmanned Ground Vehicle (UGV), capable of performing soil sample acquisition and delivery, and a multirotor Unmanned Aerial Vehicle (UAV), providing to the UGV and human experts an aerial perspective of the operation site. Via custom drilling tools, the robotic team is able to extract up to 9 cylindrical

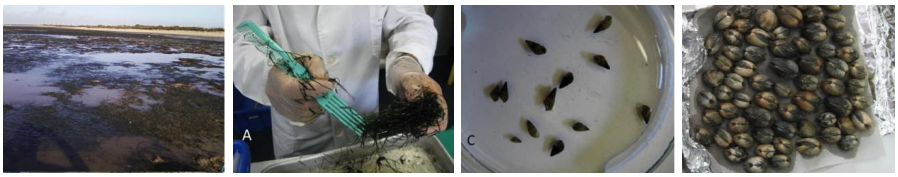

(a) (b) (c) (d)

Fig. 2. Biota at Tagus river's estuary mudflats. (a) Mudflat covered with seagrass. (b) Working on a sample of seagrass *Z. noltii*. (c) small gastropods removed from the seagrass' stems. (d) A clam (*R. philippinarum*) sample.

soil samples, each with a section of 6 cm and a depth of 45 cm. A solution based on a robotic arm manipulating smaller sampling containers (e.g., [3]) would not be able to reach such sample depth and volume, hampering offline analysis in non-emergency scenarios. Self-burying robots (e.g., [4, 5]) are a promising alternative to drilling tools, yet, it is still unclear how these robots can extract sample volumes for sufficiently significant routine radiological monitoring.

The ability to sample near-the-surface seaweeds is also key, as they supply organic food to a variety of dependent food webs and act as nursery ground for animal species [6]. Sampling clams is also relevant as these can influence human health directly. Bearing this in mind, the herein proposed robotic team is equipped with a second extraction tool adapted to sample seaweeds and clams.

The robotic team is a sampling tool, which, as other sampling tools, must be properly encompassed by experimental protocols. Consequently, this paper adapts well established environmental monitoring experimental protocols to exploit the robotic system's capabilities and to demonstrate the robotic system as an environmental survey robotic tool, contributing to the monitoring of the actual distribution patterns of radionuclides and heavy metals in an estuarine bay.

This paper is organised as follows. Section 2 presents the use-case that motivates the experimental protocol described in Section 3. Then, the robotic system, developed bearing into account the experimental protocol, is presented in Section 4. Finally, some conclusions and future work avenues are drawn in Section 5.

2 A motivating example: the Tagus river's estuary

The specification, development, and validation of the robotic system relies on Tagus river's estuarine bay as the main case-study (see Fig. 2(a)). The selection of this case-study stems from two main observations. First, as it will be shown below, studying Tagus' estuary is a remarkably relevant problem from an environmental monitoring standpoint. Second, Tagus' estuary is representative of a vast set of estuaries influenced by major littoral cities, such as Lisbon.

The muddy sediments of the Tagus river's estuary have been exposed to decades of contaminants' deposition from local industries. The runoff and wind

spreading of particulate materials coming from the phosphogypsum stockpile of a disabled phosphate plant, near the city of Barreiro, have been a source for localised enhanced concentrations of natural radioisotopes of the uranium family. Phosphogypsum is an industrial waste primarily resulting from phosphate rock reacting with sulphur acid to produce phosphoric acid. Uranium rich phosphate rock from the north of Africa was used in the plant, so the waste product has enhanced levels of radionuclides form the uranium decay series, usually classified as Normally Occurring Radioactive Material (NORM). The radiological impact of the Barreiro phosphate industry due to uranium 238 descendants, lead 210, and polonium 210, in the bottom sediments and in the water column particulate matter has been described in [7].

Other industries set on both sides of the estuarine bay contributed to the dispersion of toxic metals like mercury, cadmium or arsenic, and a variety of other different contaminants including Polycyclic Aromatic Hydrocarbons (PAH) and organometallic compounds that have been previously reported suggesting a deterioration of water and sediment quality in some critical areas of the Tagus estuary [7]. The construction of the Vasco da Gama Bridge (roughly 25 km upstream the estuary mouth), from September 1994 to December 1998, caused additional disturbance, promoting the remobilisation of anoxic contaminated sediments. This fact led to the temporary solubility of toxicant metals followed by re-adsorption to the particulate phase [8].

The decade 2000-2010 was a time for some observable changes in both the presence of human activity and the physiognomy of the estuarine mudflat extending through the shoreline from Barreiro to Alcochete. The introduction of the invasive Asian clam *Ruditapes philippinarum* (Fig. 2(d)) and its massive population expansion triggered an intense activity of clam harvesting for human consumption without any control of toxicants. At the same time, a notorious and progressive green coverage of several areas of the mudflat could be witnessed. The sea grass *Zostera noltii* (see Fig. 2(a) and Fig. 2(b)) was then identified in the course of an exploratory sampling initiative and appeared to be the residence substrate for small gastropods (see Fig. 2(c)). There is also evidence about the presence of squids.

In sum, there are several factors potentiating the presence of radionuclides and heavy metals in the estuarine bay, which, in turn, contaminate the food-chain that ultimately impacts human health. The robotic team herein presented is expected to foster accurate spatio-temporal soil and biota sampling so that environment researchers can study these phenomena in detail.

3 The Experimental Protocol

The sampling procedure will follow the principle of transect sampling generally described by the International Commission on Radiation Units and Measurements, for the purpose of estimating spatial distribution patterns of radionuclides in large areas with closely spaced sampling locations [9]. All actions performed by the robotic system will be the result of the fine tuned interaction of both aerial

and terrestrial devices, the latter being capable of acting accordingly to the information transmitted by the former, and also in the context of human-robot interaction to the direct instructions of an operator.

3.1 Chain of robot-assisted tasks

During a sampling process in the estuarine mudflat, the operational tasks will be performed according to the following sequence (refer to Fig. 3 for a graphical representation of each of the following steps):

1. The aerial robot takes off and performs a scan on the operational area defined by the user. The result is a high resolution geo-referenced mosaic built from a set of mutually registered aerial images. On top of this aerial mosaic, the system (assisted by the human operator) maps potential dead-ends, safe paths, and sampling points.
2. At the control centre, the high resolution mosaic is segmented, either manually or automatically, so as to obtain the main features of the estuary to be sampled. Water ponds and channels, sea grass coverage, salt marsh vertical vegetation, sand banks, and all sorts of physical obstacles are examples of such features. Based on the segmented aerial mosaic, the user prepares the mission by specifying a set of transects to be sampled by the robot.
3. With the information collected in 2, the ground robot traverses the transects and periodically samples the terrain. While moving, the robot avoids unexpected obstacles and sends current telemetry data to the control station. From there, the user supervises the robots' operation and sends corrective commands whenever required. At each sampling point, the ground robot extracts the terrain samples while the UAV provides images augmenting the operator perception about the current mission.
4. When the robot has either its reservoir filled-out, or visited all the pre-defined sampling locations, it returns to the base. The user operator may help the robot with this procedure.
5. Back on the base, the robot unloads the sample containers into isothermal boxes with cooling pads. This way, the samples are kept frozen until they are brought to the lab for post-processing.
6. The robot executes a process of self-washing to clean its sensors and tools.
7. Finally, the robot is recharged with empty collectors for a new mission. At this point, the user may be called upon to execute some maintenance procedures, such as recharging batteries or re-inflate tyres.

3.2 Sampling procedures

A proper sampling campaign must ensure that samples are both spatially distributed, and their volume is sufficient for the subsequent offline analysis to provide significant results. In non-emergency radiological situations the density of contaminants per sample is low. As a consequence, large sample volumes are

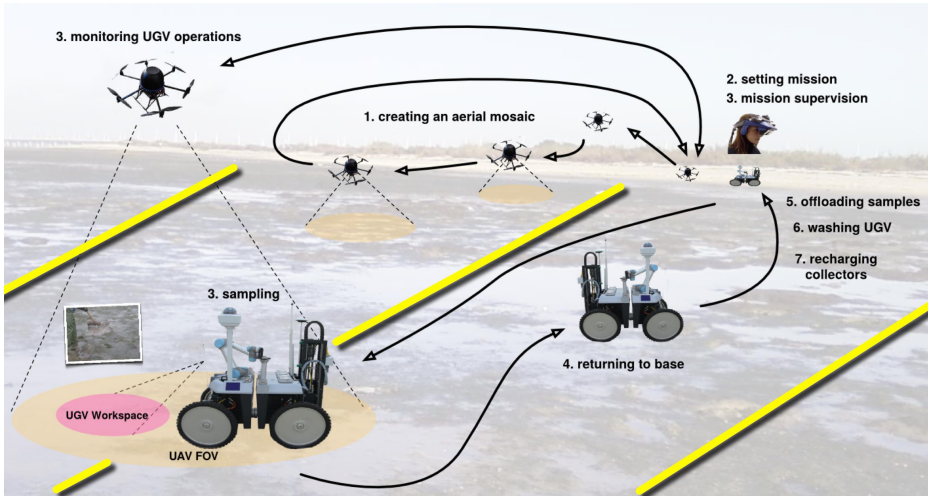

Fig. 3. Diagram representing a typical mission work-flow, whose sequence is represented by the illustrated enumeration. Tasks with the same enumeration run in parallel. Robot's motion is represented by the black curved arrows. The yellow thick lines depict the transects to be executed by the robot.

required if contaminants are to be detected therein. The following paragraphs specify the volumes for a typical radionucleids and heavy metals characterisation.

Sediment cores are extracted both in bare and sea grass covered mudflat, to support a posteriori partition analysis of metal and radionuclides in sediments and sea grass. For each sampling location, 500 m long transversal transects are defined perpendicularly to the shore line. The ground vehicle stops every 100 m along the transect. Each stopping position defines the centre of a circular sampling area with 6 m diameter, from which 9 sediment cores (45 cm depth and 6 cm diameter) are randomly extracted by the robot.

Sea grasses and bivalves are collected with the grid-like dredgers present in the ground vehicle. Sea grass sampling is done by dredging along 100 m transects defined on the sea grass bed, desirably accumulating no less than 2 kg, including attached sediments and debris. Bivalves resident in the upper layers of the bottom sediments are collected similarly. The path extension has necessarily to be larger than for sea grass sampling and the procedure must be executed in several trials until an amount of 4 kg is reached (including attached sediments and debris).

3.3 Sample processing

At the lab, the cores are unfrozen and sectioned in depth layers (0 cm − 5 cm; 5 cm − 15 cm; 15 cm − 25 cm; 25 cm − 35 cm; 35 cm − 45 cm) and all sections of a specified depth range are mixed into a composite sample. Composite samples from specified depth layers are oven dried at a temperature of 60 °C. The fine

grain size fraction composed of silts and clays are separated from sand particles in a mechanical sieving system (silt, clay $< 64\,\mu$m, sand $< 200\,\mu$m). Samples are kept dried in tagged plastic containers for further radiological and trace metal analysis.

Fresh seagrasses are washed and rinsed in water for the removal of attached sediments, debris (shell fragments, stones, etc.) and small invertebrates. Clean subsamples are separated for fresh/dry weight measurements. All samples are oven dried at $60\,^{\circ}$C, homogenised in a knife mill to a small particle size and kept dried in plastic containers.

Fresh bivalves are washed and rinsed in water and then kept frozen in tagged plastic containers. Individual size classes are determined by biometric analysis of shells' samples. Samples are processed by unfreezing the individuals and separating edible parts from shells. Unfrozen edible parts are weighed fresh and freeze dried. The dried edible parts are homogenised in a knife mill and shells are crushed and homogenised in a cutting mill. Dried samples of edible parts and crushed shells are kept in tagged plastic containers for further analysis.

4 The Robotic System

This section describes the two unmanned vehicles that compose the proposed robotic team. The robots have been devised in order to meet the requirements imposed by the experimental protocol presented in Section 3.

4.1 Mission Control

For improved interoperability, the whole robotic system runs on top of the Robot Operating System (ROS) [10]. ROS provides a publish-subscribe inter-process messaging service on top of a master-slave communications framework. To avoid a single point of failure, a multi-master configuration is used by including the *rosbridge* extension [11]. Additionally, *rosbridge* provides a JSON API to ROS functionality, which enables interoperability between robots and control centre over web-based communication channels.

The control centre is based on a Getac V200 with an Intel Core i7-620LM 2.0 GHz and 4 GB of RAM. The laptop docks onto the control centre allowing it to charge and establish a secure communication path to the robots. Two joysticks allow the smooth and precise control of the robot and pan-tilt-zoom camera. A $1200\,\mathrm{cd/m^2}$ sunlight readable display allows the user to supervise in real-time the robots' progress.

4.2 The Unmanned Ground Vehicle (UGV)

The UGV is a $1100 \times 1525 \times 1368$ mm (width x length x height) four-wheeled based on the general-purpose INTROBOT robotic platform [12]. Its front and rear wheels are decoupled through a passive longitudinal joint so as to comply with uneven and muddy terrain (see Fig. 1(a)). The robot's chassis is made of

aluminium alloy to reduce weight and increase durability and thermal conductivity. To prevent corrosion caused by salt water, the robot is covered with an hydrophobic coating. Several parts, such as the robot's top covers, are made of composite materials in order to achieve the lowest weight possible while still offering the required robustness. With payload, the overall weight of the robot amounts to 240 kg.

The UGV is equipped with individual 250 W steer and 550 W drive motors, providing quasi-omnidirectional locomotion capabilities. The robot is able to move in Ackerman and double Ackerman configurations, to rotate around its own centre (see Fig. 1(a)), and to move linearly in a wide range of directions without rotation. This multi-modal locomotion becomes of special importance whenever the robot needs to make fine adjustments to its pose to, for instance, align its drilling tool to a specific sampling spot. The wheels have a diameter of 0.3 m and a nominal section width of 0.1 m. The wheels are partially deflated to two thirds of their recommended pressure so as to increase the tyres footprint and, consequently, reduce the chances of slippage in sand and mud. Although deflating the tyres is expected to largely solve the slippage problem in estuarine environments, we are currently assessing whether tyres with larger nominal width would not provide a more robust and energetically efficient solution.

Interchangeable sampling tools can be appended to the robot's rear. Currently, two tools are available, one for drilling the terrain for soil samples and another for dredging seaweeds and clam (see Fig. 4). An actuator in the drilling tool revolves a cylindrical hollow metallic tube with internal section 45 mm and length 500 mm, which is simultaneously pushed downwards by a linear actuator. The whole drilling process takes roughly 60 sec. To cope with the contingency of drilling in surfaces with buried hard elements (e.g., rocks), the linear actuator's current and position is monitored continuously throughout the process. A similar linear actuator is also used in the dredging tool. In this case, the linear actuator pushes a 1.4 cm^3 dredger towards the ground, which is then filled with seaweeds and clam by moving the robot forwards.

An Universal Robotics UR5 compliant robotic arm with 6 degrees of freedom is responsible for autonomously moving the hollow metallic tubes and dredger between their storage sockets and their corresponding sampling tools. The compliance characteristics of the robotic arm are crucial to ensure the safety of people working in the robot's vicinity. The ground vehicle is able to store 9 hollow metallic tubes and 4 dredgers. Once the available containers are filled, the soil samples in the hollow metallic tubes must be removed as a pack, that is, without mixing soil from different depths. To facilitate this task, each hollow metallic tube encompasses two half-hollow PVC tubes (separated longitudinally), which easily slide out of the metallic tube with the help of an operator. Fig. 5 depicts a sampling sequence, from setting the hollow tube in the drilling tool to the point when the expert removes the sample's inner PVC container.

The robustness of the robotic platform and its payload was validated with a standard finite element analysis in SolidWorks. Quantitative results are not herein provided due to space limitations. Energy is supplied by eight lithium

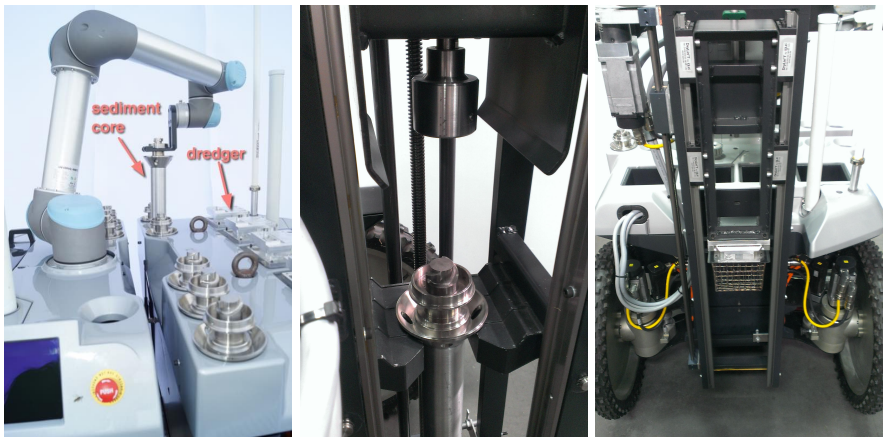

(a) (b) (c)

Fig. 4. (a) The robotic arm grasping a hollow tube to insert it into the drilling tool. (b) An hollow tube being attached to the drilling tool. (c) A dredger being pushed downwards by the dredging tool.

ion cells with a total capacity of 100 Ah, allowing more than 4 hours of operation. Robot's inter-process communications are ensured by a gigabit Ethernet, whereas wireless communications are available via Ubiquiti airMAX 2.4/5.0 GHz dual-band and a GSM uplink. This setup enables communications up to 1 km in the mudflat, under line of sight.

A SICK LMS111 2D laser scanner mounted on a Robotis Dynamixel tilting unit and a pair of DragonFly cameras for stereo-vision deliver 3D point clouds, which are integrated onto a probabilistic octree [13]. Localisation is estimated with an Extended Kalman Filter, fed by a PhidgetSpatial Inertial Measurement Unit (IMU), from Phidgets, and a GPS-RTK Proflex 800, from Ashtec SAS. Motion planning is carried out using conventional motion and path planning techniques [14] operating on a cost map [15].

4.3 The Unmanned Aerial Vehicle (UAV)

The aerial team member, the UAV, was designed to withstand the difficult operational environment of estuarine environments, where robustness and reliability are key. Taking this into account, a 6-rotor configuration with vertical take-off and landing capabilities was chosen (see Fig. 1(b)). This configuration combines a good thrust-to-weight ratio and redundancy to enable safety landings in the event of a malfunctioning motor.

The UAV's control system is supported by two computational units, one dedicated to low-level motion control and, the other, to high-level mission execution functions. Communication between controllers is assured by the MAVLink Micro Air Vehicle Communication Protocol. The low-level control unit is a VRBrain

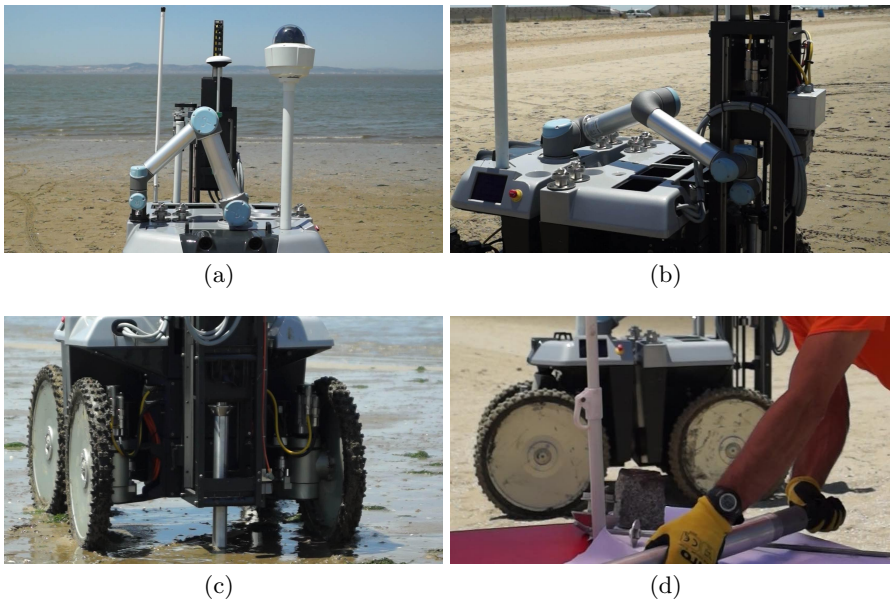

Fig. 5. Sequence of a sampling run. (a) The robot's 6-DOF arm grasps one hollow tube to be used as a soil sediments container. (b) The container is then placed on the drilling tool. (c) The tool begins drilling to obtain a core sample. (d) The half-hollow PVC inner tube being removed from the outer hollow metallic tube.

from Virtual Robotix, interfaced with an on-board IMU based on the MPU6500, a MS5611 barometer, and a GPS device from Ublox. These sensors are Kalman-filtered for pose estimation. The high-level functions are ROS-enabled and run on the top of a Xubuntu's 14.04 lightweight Linux distribution. The computational unit supporting high-level functions is an Odroid-XU from Hardkernel equipped with an Exynos octa-core CPU.

The low-level stabilisation and basic navigation software is assured by a modified version of the open-source Arducopter platform, whereas high-level navigation and interaction features are handled by dedicated ROS nodes. To take aerial images, which support the creation of aerial mosaics for a proper mission planning, the UAV uses a SJ4000 camera with diagonal 170 ° field of view mounted on an active gimbal. Communications with the UGV and the control centre are ensured by a 2.4 GHz Ubiquiti Picostation.

The main function of the UAV is to autonomously execute a line-sweep pattern so as to build an aerial mosaic of a designated operational area. As can be seen in Fig. 6, the mosaic's appearance differs greatly from the satellite imagery of the same site, which clearly shows the value of relying on up-to-date imagery taken by the UAV. The UAV takes a set of aerial images, which are then registered to each other to build up an aerial mosaic using the Hugin Panorama open-source software [16]. Then, this aerial mosaic is used to specify the sam-

(a) (b)

Fig. 6. An aerial mosaic, built by the UAV, of an operations site nearby Samouco, in the south margin of Tagus' estuary bay. (a) Satellite imagery of the site with UAV's executed path overlaid. (b) The resulting aerial panorama.

pling mission by the operator in the control centre. Currently, the user simply specifies the transects by visually analysing the mosaic. In the future, we expect to include automated terrain classification algorithms to aid the operator in this task. Once this initial process is completed, the UAV lands and waits for additional user-requested monitoring of the UGV's sampling activity.

5 Conclusions

A ground-aerial robotic team for soil and biota sample collection and retrieval in estuarine mudflats, was presented. To frame the robotic system in radionucleids and heavy metals environmental monitoring campaigns, a preliminary experimental protocol tailored to exploit the capabilities offered by the robotic system was also proposed. A set of preliminary field trials in Tagus' estuarine bay showed the ability of the robotic system prototype to navigate, extract samples, and retrieve them for subsequent offline analysis. We are currently preparing a full environmental monitoring campaign to validate the proposed experimental protocol and further assess the robustness and accuracy of the robotic system when facing the burdens of long field operations. As future work, the robotic system will be extended so as to include water surface unmanned vehicles for joint water/land sampling. The experimental protocol will also be adapted to account for the extended robotic team.

6 Acknowledgement

This work was co-funded by ROBOSAMPLER project (LISBOA-01-0202-FEDER-024961). The authors wish to thank the fruitful comments provided by the anonymous reviewers.

References

1. Eggleton, J., Thomas, K.V.: A review of factors affecting the release and bioavailability of contaminants during sediment disturbance events. Environment international **30**(7) (2004) 973–980
2. Murphy, R.R., Peschel, J., Arnett, C., Martin, D.: Projected needs for robot-assisted chemical, biological, radiological, or nuclear (cbrn) incidents. In: Proc. of the IEEE International Symposium on Safety, Security, and Rescue Robotics (SSRR), IEEE (2012) 1–4
3. Guzman, R., Navarro, R., Ferre, J., Moreno, M.: Rescuer: Development of a modular chemical, biological, radiological, and nuclear robot for intervention, sampling, and situation awareness. Journal of Field Robotics, DOI: 10.1002/rob.21588 (2015)
4. Winter, A.G., Deits, R.L., Dorsch, D.S., Hosoi, A.E., Slocum, A.H.: Teaching roboclam to dig: The design, testing, and genetic algorithm optimization of a biomimetic robot. In: Proc. of the IEEE/RSJ International Conference on Intelligent Robots and Systems (IROS), IEEE (2010) 4231–4235
5. Darukhanavala, C., Lycas, A., Mittal, A., Suresh, A.: Design of a bimodal self-burying robot. In: Proc. of the IEEE International Conference on Robotics and Automation (ICRA), IEEE (2013) 5600–5605
6. Larkum, A., Orth, R.J., Duarte, C., eds.: Seagrasses: Biology, Ecology and Conservation. Springer (2006)
7. Carvalho, F.P., Oliveira, J.M., Silva, L., Malta, M.: Radioactivity of anthropogenic origin in the tejo estuary and need for improved waste management and environmental monitoring. International Journal of Environmental Studies **70**(6) (2013) 952–963
8. Caetano, M., Madureira, M.J., Vale, C.: Metal remobilisation during resuspension of anoxic contaminated sediment: short-term laboratory study. Water, air, and soil pollution **143**(1-4) (2003) 23–40
9. ICRU: Sampling to estimate spatial pattern. Journal of the ICRU **6**(1) (2006) 49–64
10. Quigley, M., Gerkey, B., Conley, K., Faust, J., Foote, T., Leibs, J., Berger, E., Wheeler, R., Ng, A.: Ros: an open-source robot operating system. In: Proc. of the ICRA Open-Source Software Workshop. (2009)
11. Mace, J.: Rosbridge. `http://wiki.ros.org/rosbridge_suite` (2015) Accessed: 2015-09-07.
12. Marques, F., Santana, P., Guedes, M., Pinto, E., Lourenço, A., Barata, J.: Online self-reconfigurable robot navigation in heterogeneous environments. In: Proc. of the IEEE International Symposium on Industrial Electronics (ISIE), IEEE (2013) 1–6
13. Wurm, K.M., Hornung, A., Bennewitz, M., Stachniss, C., Burgard, W.: Octomap: A probabilistic, flexible, and compact 3d map representation for robotic systems. In: Proc. of the ICRA 2010 workshop on best practice in 3D perception and modeling for mobile manipulation. Volume 2. (2010)
14. Gerkey, B.P., Konolige, K.: Planning and control in unstructured terrain. In: Proc. of the IEEE ICRA Workshop on Path Planning on Costmaps. (2008)
15. Lourenço, A., Marques, F., Santana, P., Barata, J.: A volumetric representation for obstacle detection in vegetated terrain. In: Proc. of the IEEE Intl. Conf. on Robotics and Biomimetics (ROBIO), IEEE Press (2014)
16. D'Angelo, P.: Hugin-panorama photo stitcher. `http://hugin.sourceforge.net` Accessed: 2015-09-07.